

RSC Advances



This is an *Accepted Manuscript*, which has been through the Royal Society of Chemistry peer review process and has been accepted for publication.

Accepted Manuscripts are published online shortly after acceptance, before technical editing, formatting and proof reading. Using this free service, authors can make their results available to the community, in citable form, before we publish the edited article. This *Accepted Manuscript* will be replaced by the edited, formatted and paginated article as soon as this is available.

You can find more information about *Accepted Manuscripts* in the [Information for Authors](#).

Please note that technical editing may introduce minor changes to the text and/or graphics, which may alter content. The journal's standard [Terms & Conditions](#) and the [Ethical guidelines](#) still apply. In no event shall the Royal Society of Chemistry be held responsible for any errors or omissions in this *Accepted Manuscript* or any consequences arising from the use of any information it contains.

Cite this: DOI: 10.1039/c0xx00000x

www.rsc.org/xxxxxx

PAPER

Silica nanospheres supported diazafluorene iron complex: an efficient and versatile nanocatalyst for the synthesis of propargylamines from terminal alkynes, dihalomethane and amines

R.K. Sharma*, Shivani Sharma and Garima Gaba

5 Received (in XXX, XXX) Xth XXXXXXXXXX 20XX, Accepted Xth XXXXXXXXXX 20XX
DOI: 10.1039/b000000x

We present the synthesis of an efficient heterogeneous silica nanospheres supported iron catalyst (SiO₂@APTES@DAFO-Fe) and its catalytic application in one pot three-component coupling reaction of terminal alkynes, dihalomethane and secondary amines for the facile synthesis of propargylamines. The synthesized SiO₂@APTES@DAFO-Fe nanocatalyst has been systematically characterized by Solid-state ¹³C CPMAS and ²⁹Si CPMAS NMR spectroscopy, Fourier transform infrared spectroscopy (FT-IR), Transmission electron microscopy (TEM), Brunauer–Emmett–Teller (BET) surface area analysis, Scanning electron microscopy (SEM), Atomic absorption spectroscopy (AAS), Energy dispersive X-ray fluorescence spectroscopy (ED-XRF), and elemental analysis. The nanocatalyst exhibits high catalytic performance for the coupling reaction of aromatic terminal alkynes, dichloromethane and secondary amines to afford propargylamines. In order to achieve high catalytic efficacy, the effect of various reaction parameters such as temperature, base, the amount of catalyst, reaction time, type of solvent, substrate molar ratio etc. have been investigated. Furthermore, the recovery and reuse of the quasi-homogeneous nano-catalyst have been demonstrated several times without any appreciable loss in its catalytic activity. Apart from this, FT-IR, SEM and HRTEM techniques are employed in order to prove the stability of the reused nano-catalyst. The present protocol works under mild reaction conditions with the additional advantages of simple work-up procedure, high product yield, and easy recovery and reusability of the nanostructured catalyst. It is noteworthy that this atom economical methodology does not require an additional co-catalyst or activator. A tentative mechanism is also proposed for the one pot coupling reaction for the synthesis of propargylamines.

Introduction

The development of new green and sustainable technology for various chemical transformations has recently gathered a great deal of attention because it represents a new strategy to meet the challenges of energy and sustainability.^{1,2} One effective way to surmount these challenges is to employ a highly efficient and stable catalyst for the synthesis of fine chemicals, especially under eco-friendly and safe reaction conditions. Homogeneous catalytic system serves as a powerful and versatile tool for various organic synthesis enabling good control of reactivity with chemo-, regio- and stereoselectivity as it allows easier and greater interaction between the components. However, despite these significant features, its widespread application in practical and process chemistry is still hampered due to associated drawbacks of high costs, multi-step preparation and difficult separation from the reaction mixture.³⁻⁶ On the contrary, the economic advantages of heterogeneous catalysis such as excellent stability, facile catalyst handling and separation from the reaction mixture have also increased its competence in industrial organic transformations despite having low activity and selectivity in

comparison to homogeneous catalysis.⁷ To conquer the problems associated with both homogeneous as well as heterogeneous catalysts, chemists and engineers have investigated a wide range of strategies amongst which the covalent immobilization of catalytically active species onto various solid supports appears to be the best logical solution.^{8,9} The heterogenization of the existing homogeneous catalyst can potentially provide novel recyclable and reusable solid catalysts that have uniform and precisely engineered active sites similar to their homogeneous counterparts, and therefore preserve the desirable attributes of both the systems.¹⁰⁻¹³ This strategy not only reduces the loss of catalyst, but also enhances reusability, making the catalyst cost-effective and promising for wide industrial applications. Over the past few decades, there have been extensive reports on the heterogenization of soluble catalysts using various solid support materials such as metal oxides, polymers and nanocomposites.¹⁴⁻¹⁹ In this context, nanomaterials as a solid support have conquered new horizons in the field of catalysis due to their intriguing properties such as large surface area, excellent stability and high complex loading in comparison to bulk materials. It is well evident from literature that the novel heterogenized catalysts are

based on silica nanospheres as a solid support, primarily because they display some advantageous properties, such as nanometre size, excellent chemical and thermal stability, good accessibility, porosity, and large surface area to volume ratio.²⁰⁻³¹ Besides, the abundant silanol groups on their surfaces make them easily organically functionalized by different post-synthetic modifications so as to provide active catalytic centers. Remarkably, these quasi-homogeneous catalysts are devoid of diffusion problems as they can be easily dispersed in several solvents which facilitate the accessibility of the reactants to the catalytic active sites.

Within this framework a novel silica nanospheres supported iron catalyst has been prepared for the three component coupling reaction of aromatic terminal alkynes, dichloromethane and secondary amines to furnish propargylamines. The synthesis of propargylamines is one of the most significant transformations from both synthetic and industrial points of view, since propargylamines are synthetically adaptable key intermediates for the production of many nitrogen-containing biologically active compounds such as conformationally restricted peptides, oxotremorine analogues, β -lactams, isosteres, therapeutic drug molecules, sedative, hypnotic, antispasmodic, analgesic, and anti-inflammatory effects.³²⁻³⁷ Traditionally, propargylamines synthesis was achieved via three component coupling reaction of aldehydes, alkynes, and amines catalyzed by various transition metals. However, Contel et al. has recently reported gold catalyzed three-component coupling reaction of alkynes, haloalkanes and amines to furnish propargylamines, wherein new C–C and C–N bonds are constructed via the activation of C–H and C–halogen bonds.³⁸ Besides, Cu(I), nano-In₂O₃, Fe(III), Ni(II) and cobalt have also been reported to catalyze the concerned coupling reaction.³⁹⁻⁴⁴ Unfortunately, these existing synthetic methodologies suffer from numerous shortcomings such as longer reaction times, harsh reaction condition, low product yield, lack of atom economy and tedious workup procedure which render them environmentally unsafe and limit their large scale operation. Moreover, metal contamination of the products is inevitable during the process of extraction of the reported homogeneous catalysts. Therefore, design and development of improved synthetic method for the preparation of propargylamines is highly desirable for industrial application.

Considering the need for a better catalytic system that would uniquely combine the best features of both homogeneous and heterogeneous catalysts, we have developed silica nanospheres based palladium catalyst for the oxidative amination of aldehydes under solvent free condition using hydrogen peroxide as a sole environmentally benign oxidant.⁴⁵ Thus, in continuation of our ongoing research work on the development of green and sustainable synthetic pathways for organic-inorganic hybrid materials, and their applications as metal scavengers, sensors, and catalysts for various organic transformations⁴⁶⁻⁵⁷, herein we report the synthesis, characterization and application of novel silica nanospheres supported diazafluorene iron catalyst for three-component coupling reaction of aromatic terminal alkynes, dichloromethane and secondary amines to afford propargylamines via C–H and C–Cl bond activations. Notably, the nanocatalyst exhibits high activity and a wide range of substrate applicability. Further, this nanocatalyst also displays

excellent durability and can be reused several times with negligible loss of its catalytic activity. Hence, this one pot protocol overcomes the traditional drawbacks of the reported homogeneous catalysts and has a good prospect for its wide scale application.

Experimental

Materials and reagents

Tetra-ethyl orthosilicate (TEOS) (99.9%) (Sigma Aldrich), 3-aminopropyltriethoxysilane (APTES) (98%) (Fluka), Ferric chloride (Sisco Research Laboratory) and diazafluorene (Alfa Aesar) were commercially procured, and used as received without further purification. All other starting materials and reagents used in the reactions were obtained from Alfa Aesar and Spectrochem Pvt. Ltd, India.

Physicochemical characterizations

Fourier transform infrared (FT-IR) spectra of all samples were performed on KBr pellets by using a Perkin Elmer Spectrum 2000 FT-IR spectrometer in the 4000-400 cm⁻¹ region under atmospheric conditions with a resolution of 1 cm⁻¹. Wide angle powder X-ray diffraction (XRD) measurements were conducted for pre-dried samples by using a Bruker D8 ADVANCE (Karlsruhe, bundesland, Germany) X-ray diffractometer with Cu K α radiation and a secondary monochromator. The diffraction patterns were measured in the high angle region (2 θ scanning range from 10° to 60°). The structure and morphology of the nanomaterials were verified by high resolution transmission electron microscopy (HRTEM) (TECNAI G2 T30 microscope) equipped with X-ray energy dispersive spectroscopy. The samples were dispersed in ethanol solution under ultrasonic vibration and one drop of the suspension evaporated onto a carbon-coated copper grid for HRTEM measurement. Energy-dispersive X-ray (EDX) analysis (equipped with the TEM instrument) was done for detailed composition characterization of the nanomaterials. The qualitative identification of free amine groups in APTES@SiO₂ was performed by the ninhydrin test. Digestion of the catalyst was done in an Anton Paar multiwave 3000 microwave reaction system equipped with a temperature and pressure sensor. Specific surface areas were determined by Brunauer-Emmett-Teller (BET) method Gemini-V2.00 instrument (Micromeritics Instrument Corp.). Samples were outgassed under vacuum at 100°C for 3 h to evacuate the physically adsorbed moisture before analysis. CHN elemental analysis was carried out using Elementar Analysensysteme GmbH VarioEL V3.00 analyzer. The amount of iron loaded on silica nanospheres was determined via flame atomic absorption spectroscopy (FAAS) on a LABINDIA AA 7000 atomic absorption spectrometer using an acetylene flame. The optimum parameters for the measurement of iron content in the sample are: wavelength = 248.3 nm; lamp current = 2 mA; slit width = 0.2 nm; fuel flow rate = 0.2 L min⁻¹. Field-emission scanning electron microscopy (FESEM) images were collected on a Tescan Mira 3 FESEM microscope; samples were coated with a gold film. GC-MS analyses of the products were performed on an Agilent gas chromatograph (6850 GC) with HP-5MS 5% phenyl methyl siloxane capillary column (30.0 m x 250 μ m x 0.25 μ m), and a quadrupole mass filter equipped 5975 mass selective

detector (MSD) using helium as the carrier gas (rate 0.9 ml min⁻¹). The temperature of the injection port was 250 °C. The temperature program of the GC column was set to an initial oven temperature of 60 °C which increased at a rate of 10 °C/min to 250 °C, and the oven was held at 250 °C for 10 min.

Fabrication of the silica nanospheres supported diazafluorene iron nano-catalyst (SiO₂@APTES@DAFO-Fe)

Firstly, monodisperse silica nanospheres (SiO₂) were synthesized via stober's method by hydrolysis of TEOS in ethanol medium using ammonium hydroxide as catalyst.⁵⁸ In a typical synthesis, 1 mL of TEOS was added into 10 mL of ethanol. Subsequently, 10 mL of 25% ammonium hydroxide and 10 mL of ethanol were also introduced to the reaction mixture synchronously under sonication which was further continued for 60 minutes to get a white turbid suspension. The reaction mixture was centrifuged in order to separate silica nanospheres which were then washed with water and ethanol respectively. After that, silica nanospheres were functionalized with APTES by the addition of 1 mL of APTES to 50 mL of a vigorously stirred dispersion of SiO₂ in ethanol, and the mixture was stirred overnight at room temperature.⁵⁹ The resulting amine functionalized silica nanospheres (SiO₂@APTES) were separated by centrifugation and re-dispersed in ethanol which was repeated three times. Next, the mixture of SiO₂@APTES and diazafluorene (DAFO) was stirred for 24 h in ethanol solution at 60 °C and the product (SiO₂@APTES@DAFO) was centrifuged and washed with

ethanol thoroughly to remove unreacted diazafluorene which was dried in a vacuum oven. Finally, SiO₂@APTES@DAFO was reacted with the solution of ferric chloride in acetone (Scheme 1) and the resulting mixture was stirred for 12 h at room temperature. The nanocatalyst (SiO₂@APTES@DAFO-Fe) was centrifuged, washed thoroughly with acetone and dried in a vacuum

General procedure of silica nanospheres supported iron nanocatalyst (SiO₂@APTES@DAFO-Fe) mediated synthesis of propargylamines

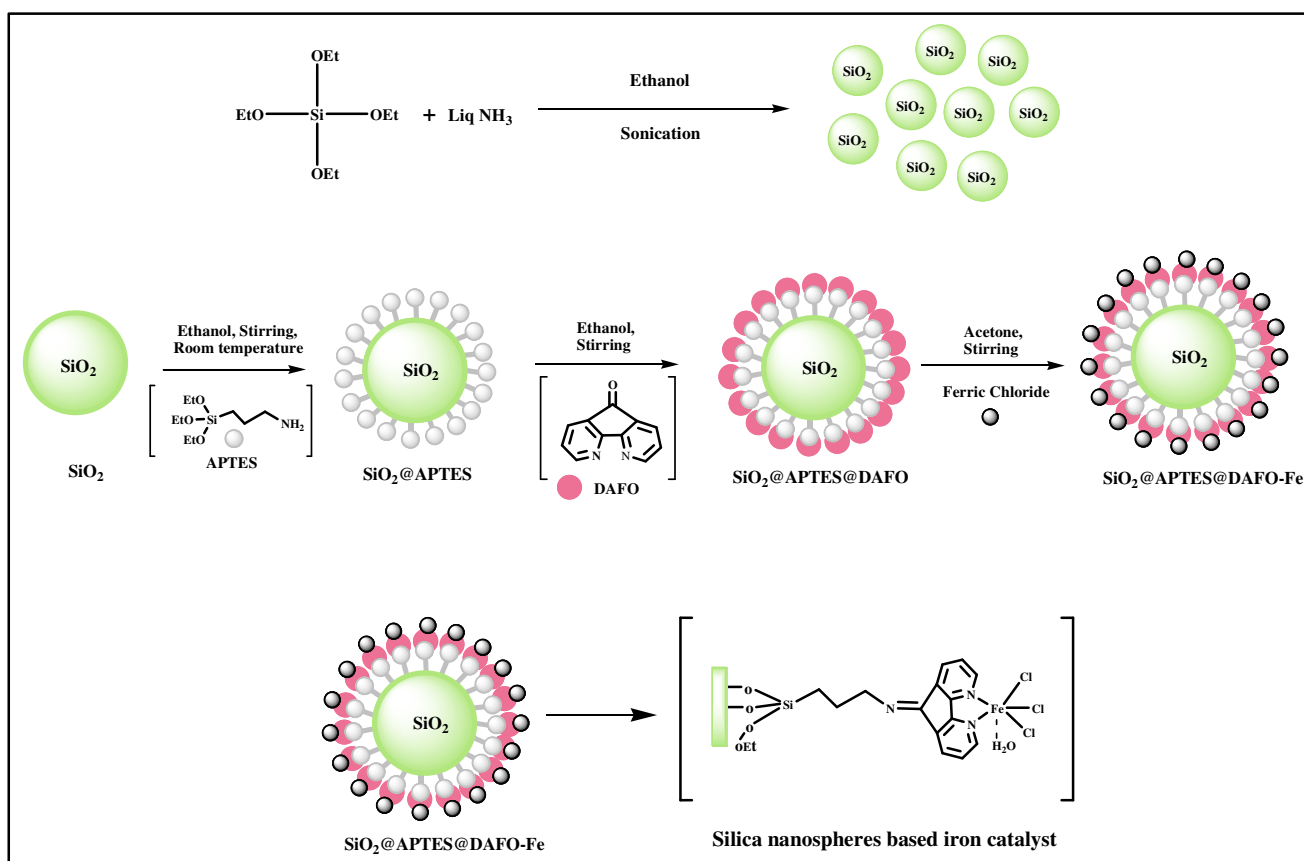
A mixture of aromatic alkynes (1 mmol), dichloromethane (2 mmol), secondary amine (2 mmol), DBU (1 mmol), 2 mL CH₃CN and SiO₂@APTES@DAFO-Fe nanocatalyst (30 mg) were refluxed at 70°C for 10 h. At the end of the reaction, the catalyst was recovered by centrifugation and washed with diethylether. The mixture was diluted with water and the aqueous layer was extracted with diethylether. The organic phase thus collected was dried over Na₂SO₄, filtered, and the solvent was removed under vacuum. The propargylamine products thus obtained were analyzed and confirmed by GC-MS.

Results and Discussion

Catalyst Characterizations

Fourier-transform Infrared spectroscopy

The FT-IR spectrum of SiO₂ exhibits characteristic vibrations of



Scheme 1 Preparation of silica nanospheres supported diazafluorene iron nano-catalyst (SiO₂@APTES@DAFO-Fe).

the silica materials related to Si-O-Si asymmetric stretching (1087 cm^{-1}), stretching vibrations of Si-OH (955 cm^{-1}), Si-O-Si symmetric stretching (802 cm^{-1}) and Si-O-Si bending vibrations (475 cm^{-1}). Moreover, the spectrum also shows H-O-H bending vibrations of physically adsorbed water at 1628 cm^{-1} and a broad band centered around 3423 cm^{-1} due to O-H stretching vibrations of hydrogen bonded surface silanol groups and physically adsorbed water. In the FTIR spectrum of the amine functionalized silica nanospheres, besides the absorption bands originated by Si-O vibrations, there are two weak bands at 2928 cm^{-1} and 2858 cm^{-1} assigned to aliphatic $-\text{CH}_2$ stretching vibrations of the propyl chain of the silylating agent (APTES) which confirm the presence of APTES onto silica surface. These results are in good agreement with the data reported in the literature.⁶⁰ Furthermore, ongoing from SiO_2 to SiO_2 @APTES, a significant reduction in the intensity of the peak from Si-OH stretching vibrations (at 955 cm^{-1}) is observed. This is because of a reaction between the surface Si-OH groups of SiO_2 and ethoxy groups of APTES during the surface modification. The spectrum of nanocatalyst shows a band at 1623 cm^{-1} indicative of the imine group resulting from Schiff condensation between the NH_2 group of SiO_2 @APTES and the carbonyl group of the ligand further provide the evidence of the grafting of the ligand onto amine functionalized silica nanospheres. FT-IR spectrum of recovered SiO_2 @APTES@DAFO-Fe catalyst after reaction was also recorded in the region $4000\text{--}400\text{ cm}^{-1}$. The spectrum of SiO_2 @APTES@DAFO-Fe after coupling reaction shows identical IR absorption bands indicating that originality of the catalyst is still retained. The recovered SiO_2 @APTES@DAFO-Fe catalyst does not show any IR bands corresponding to the organic materials suggesting that the catalyst is not poisoned during the reaction (Fig 1).

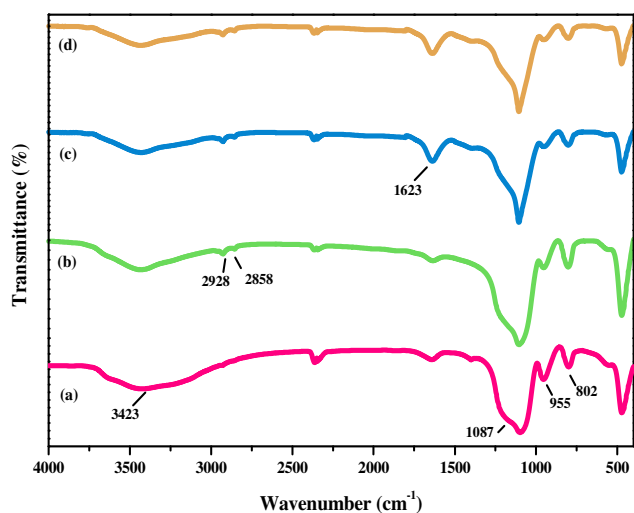


Fig. 1 FT-IR spectra of (a) SiO_2 , (b) SiO_2 @APTES and (c) SiO_2 @APTES@DAFO-Fe (d) recovered SiO_2 @APTES@DAFO-Fe

X-Ray Diffraction Studies

In order to confirm the structural characteristics of SiO_2 , SiO_2 @APTES and SiO_2 @APTES@DAFO-Fe, XRD studies were carried out, and resultant patterns are presented in Fig. 2. All silica based nanomaterials exhibit a single broad diffraction

peak at $2\theta = 23^\circ$ which is characteristic of the amorphous nature of the Stober's silica nanospheres. The results show that there is no remarkable change observed in the topological structure of silica nanospheres even after surface functionalization reactions. Hence, it may be concluded that the bare silica nanospheres are stable enough to experience the chemical modification reactions starting from the surface functionalization to the binding of iron. However, upon comparison of the diffraction patterns of these samples, decrease in XRD peak intensities of SiO_2 @APTES and SiO_2 @APTES@DAFO-Fe is observed with the successive anchoring of APTES and iron complex onto silica nanospheres. On the other hand, XRD analysis of nanomaterials does not show any novel diffraction peak. This gives a clear indication that these species existed on the surface of silica nanospheres in the form of non-crystalline state.

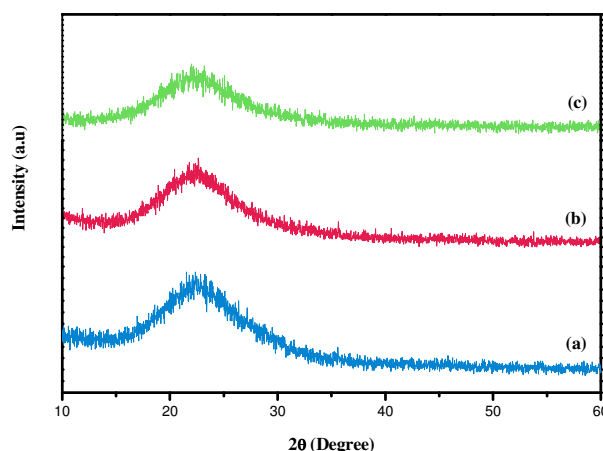


Fig. 2 XRD diffraction patterns of (a) SiO_2 , (b) SiO_2 @APTES and (c) SiO_2 @APTES@DAFO-Fe

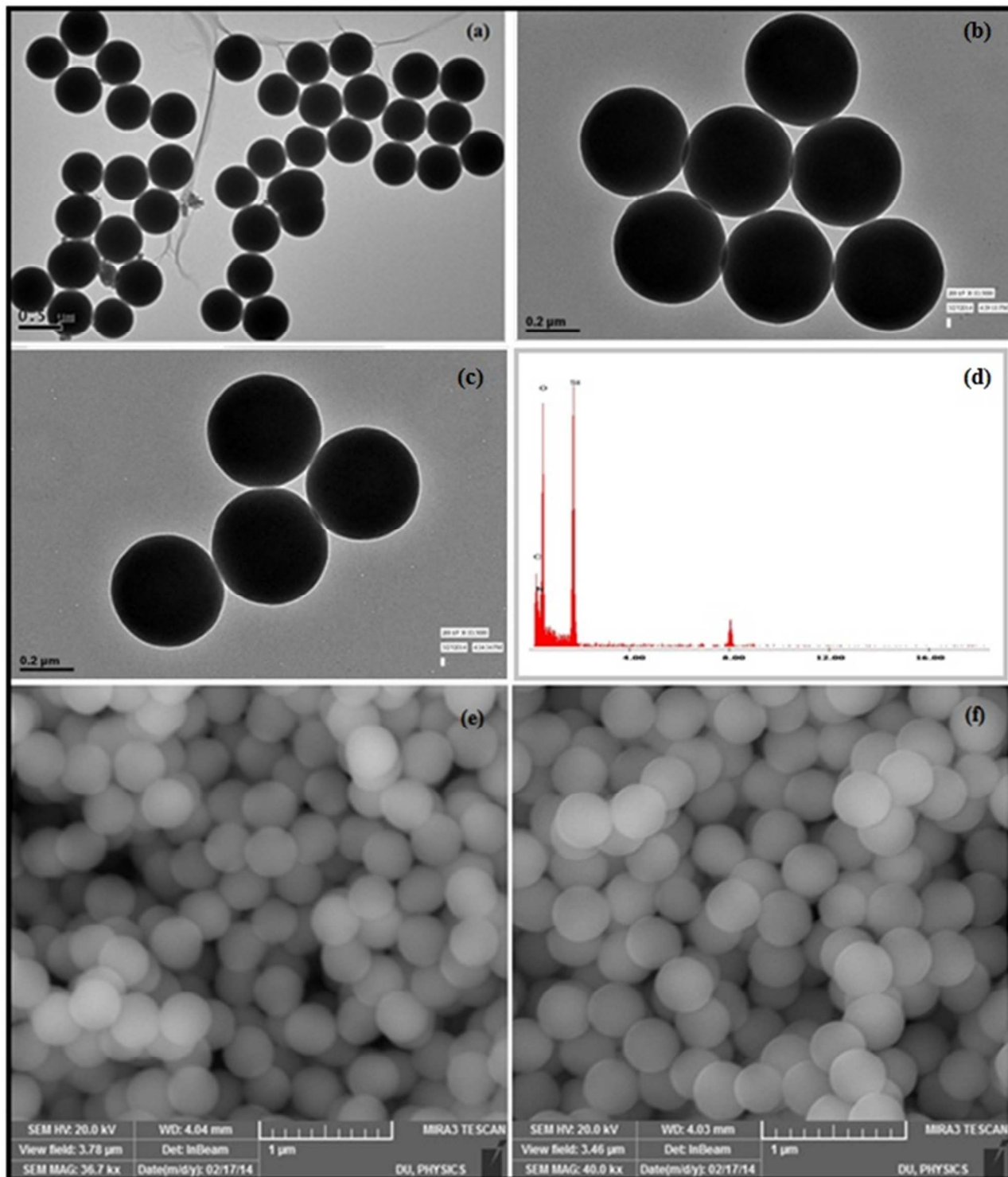
TEM and SEM analysis

The shape, size and morphologies of the synthesized nanomaterials were examined by scanning electron microscopy (SEM) and transmission electron microscopy (TEM). SEM images of functionalized as well as nonfunctionalized silica nanospheres reveal that they are monodisperse having a smooth surface (Fig. 3). TEM micrographs further confirm that these particles are spherical in shape having uniform size with an average diameter of $\sim 250\text{ nm}$. It is also evident that the morphological homogeneity that characterized these amorphous SiO_2 nanospheres is maintained even after functionalization of organic moieties. Furthermore, these particles do not agglomerate into clusters and hence leave enough surface area available on the nanoparticle for catalytic activity. EDX mapping results of SiO_2 @APTES show the presence of nitrogen species which is consistent with the presence of APTES at the surface of the SiO_2 nanospheres. Besides, TEM and SEM images of the recovered nano-catalyst after the completion of reaction have been provided which indicate that the shape and morphology of the particles remain unchanged. Hence, the catalyst is stable under the reaction conditions employed in the present work and retains catalytic activity even after recycling.

Solid state ^{13}C CPMAS and ^{29}Si CPMAS NMR Spectroscopy
 ^{29}Si and ^{13}C CPMAS solid-state NMR spectroscopy provides

useful information regarding the presence of organic moiety in the hybrid framework since the spectra of these nuclei are sensitive monitors of the silica surface and the reactants. Hence, insight into the successful modification of the SiO_2 with APTES is gained by ^{13}C CPMAS NMR spectrum of APTES@ SiO_2 as shown in Fig. 4 (a). In the ^{13}C CPMAS spectrum of the APTES@ SiO_2 , one can observe signals stemming from the alkyl

chain of APTES (10.7, 23.8, 44.2 ppm) and additionally two peaks of un-reacted ethoxy groups (16.8 and 58.1 ppm) which further confirms the covalent bonding between the silane linking group and silica nanospheres. The ^{13}C CPMAS results are in good agreement with the values reported in the literature for APTES in siliceous supports.⁶¹ Further, Fig 4 (b) represents solid state ^{29}Si NMR spectrum of SiO_2 @APTES@DAFO-Fe



15 **Fig. 3** TEM micrographs of (a) SiO_2 and (b) SiO_2 @APTES@DAFO-Fe. (c) Recovered SiO_2 @APTES@DAFO-Fe. (d) EDX spectrum of SiO_2 @APTES. (e) and SEM images of (e) SiO_2 @APTES@DAFO-Fe. (f) Recovered SiO_2 @APTES@DAFO-Fe.

catalyst which exhibits four peaks. The first of them, at -55 ppm, may be assigned to the silicon atom of the silylating agent bound to one hydroxyl group forming the structure $C-Si(OSi)_2(OH)$. This signal is usually referred to as the T^2 signal. The second peak, at -66 ppm, is assigned to $C-Si(OSi)_3$ and corresponds to the T^3 signal. The presence of T^2 and T^3 signals confirms that the organic groups are covalently bound to the SiO_2 nanospheres. The other two less intense peaks, at -101.7 and -110.5 ppm, are attributed to inorganic polymeric structure of silica nanospheres and are assigned to $Si(OSi)_3OH$ group (Q^3) signal and free silanol group of $Si(OSi)_4$ (Q^4).

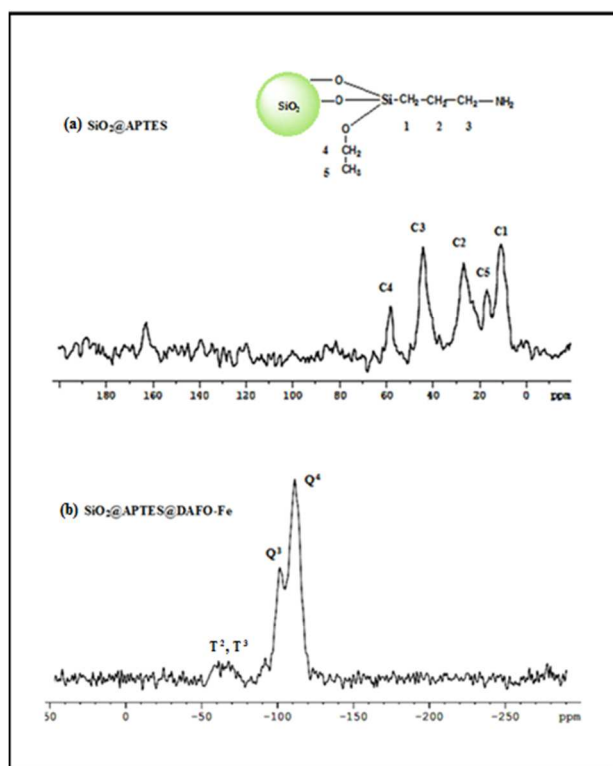


Fig. 4 (a) ^{13}C CPMAS NMR spectrum of $SiO_2@APTES$ and (b) ^{29}Si CPMAS NMR spectrum of $SiO_2@APTES@DAFO-Fe$.

Elemental and BET surface area analysis

The Brunauer-Emmett-Teller (BET) surface area measurements were also performed in order to analyze the grafting reactions and results are summarized in Table S1 (ESI †). The surface area of bare silica nanospheres was measured as 241.75 m^2 g^{-1} . However, the results reveal that there is decrease in the surface area values after successive immobilization of organic moieties. These reductions in surface areas are likely to be the result of blocking of the access of nitrogen gas molecules after the functionalization of silica nanospheres. Hence, these data provide a strong evidence of the successive anchoring of the APTES and iron complex onto the surface of silica nanospheres.⁶² Further, Ninhydrin test was also carried out in order to discover the free amino groups in the $SiO_2@APTES$ which are at the surface of solid support. Upon addition of the ninhydrin solution to the nanomaterial ($SiO_2@APTES$), change in colour from white to blue was observed, this provides clear evidence for the presence of the accessible amine groups (Fig. S1, ESI †). Next, for the

quantitative estimation of the organic functionalities present on the surface of silica nanospheres, CHN microanalysis was performed (Table S1, ESI †). The observed carbon and nitrogen contents of $SiO_2@APTES$ are 5.43 % and 1.83 % respectively. Hence, calculated C/N ratio of $SiO_2@APTES$ is found to be to be ~ 3 which matches the theoretical value, thereby confirming the APTES grafting onto the surface of SiO_2 . The nitrogen loading of $SiO_2@APTES$ was found to be 1.31 $mmol$ g^{-1} . Lastly, in order to determine the iron content in the $SiO_2@APTES@DAFO-Fe$ catalyst, quantitative analysis was performed using AAS after it was digested in nitric acid and corresponding iron loading was found to be 0.126 $mmol$ per gram of catalyst. These observations were further supported by well resolved peak of iron observed in the ED-XRF spectrum of $SiO_2@APTES@DAFO-Fe$ catalyst (Fig. 5).

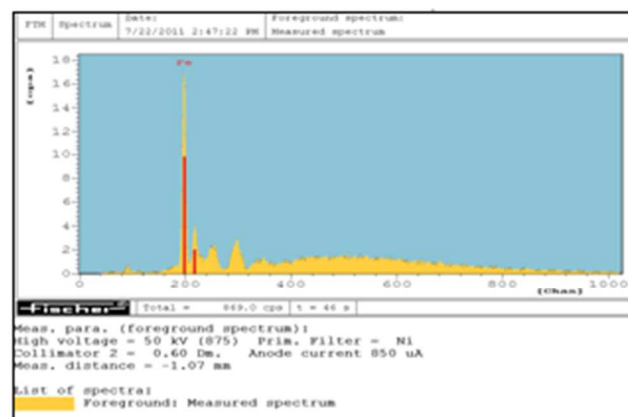


Fig. 5 ED-XRF spectrum of nanocatalyst ($SiO_2@APTES@DAFO-Fe$).

Catalytic activity tests

The catalytic efficacy of silica nanospheres supported diazafluorene iron complex ($SiO_2@APTES@DAFO-Fe$) was investigated in three component coupling reaction of terminal alkynes, halomethanes and secondary amines for the facile synthesis of propargylic amines. Initial catalytic tests were carried out in order to obtain an optimum reaction profile for coupling by varying different parameters, such as temperature, amount of catalyst, reaction time, substrate molar ratio, type of solvent and effect of bases. For that, phenyl acetylene, dichloromethane and diethylamine were chosen as the test substrates.

Screening of various catalysts

Initially, to compare the catalytic performance of the $SiO_2@APTES@DAFO-Fe$ nanocatalyst, the model reaction was performed using wide range of iron sources (Table S2, ESI †). It can be seen that the reaction did not proceed in the absence of catalyst. Similarly, the reaction did not occur with silica nanospheres alone. All of the reported homogeneous catalysts exhibited moderate activity. These homogeneous catalysts decomposed immediately after the reaction and could not be reused. On the other hand, the developed $SiO_2@APTES@DAFO-Fe$ nanocatalyst acquired the advantages of a heterogeneous catalytic system so that it could be easily recovered and reused for several catalytic cycles. In addition, the heterogeneous $SiO_2@APTES@DAFO-Fe$ nanocatalyst was

devoid of the diffusion problems because the silica nanospheres can easily be dispersed in several solvents and hence can facilitate the accessibility of the reactants to the catalytic active sites. Further, the effect of amount of the SiO₂@APTES@DAFO-Fe nanocatalyst on the conversion was also studied. The results revealed that the percentage conversion increased with an increase in the amount of the catalyst upto 30 mg. This suggests that the transition metal functions as an active site for the coupling reaction and hence with an increase in the amount of the active species the reaction becomes fast, which favours the formation of propargylic amines. A further increase in the amount of catalyst did not produce any considerable increase in the conversion because of the hindrance of the mass transfer between the active sites and reagent caused by the low dispersity of the excess catalyst in the reaction media. Thus, 30 mg of the SiO₂@APTES@DAFO-Fe nanocatalyst was found to be optimum in order to obtain maximum conversion.

Effect of temperature

Temperature is a crucial factor for the one pot three component coupling reaction. Thus, in order to determine the optimum temperature, the model reaction was performed at diverse range of temperatures (30-100°C) while keeping the other parameters fixed and the results are presented in Fig. 6. It can be seen that the conversion increased with increasing temperature from 30 to 70°C. Further increase in temperature resulted in decrease in conversion percentage probably due to the formation of small amount of dimerization product of phenyl acetylene. At 70°C highest conversion was observed and the dimerization product was suppressed. Hence, the optimum temperature for the one pot synthesis of propargyl amines was 70°C and further studies were carried out at 70°C in the presence of 30 mg of SiO₂@APTES@DAFO-Fe catalyst.

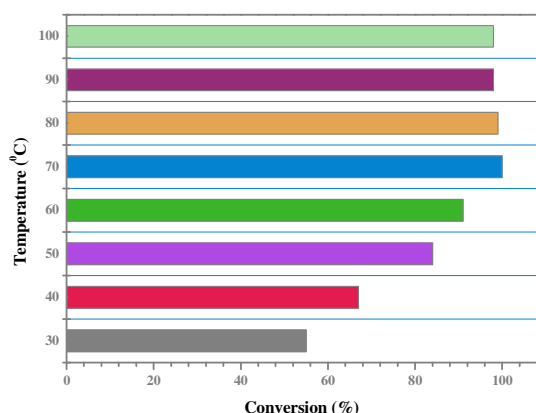


Fig. 6 Effect of temperature on model reaction (Reaction conditions: phenyl acetylene (1 mmol), dichloromethane (2 mmol), diethylamine (2 mmol), DBU (1 mmol), acetonitrile (2 mL), catalyst (30 mg), time 10 h)

Effect of various solvents and bases

Noting the importance of base in the reaction, various organic as well as inorganic bases were screened such as 1,8-diazabicyclo[5.4.0]undec-7-ene (DBU), triethylamine (TEA) and 1,4-diazabicyclo[2.2.2]octane (DABCO), K₂CO₃ and K₃PO₄ using series of solvents such as dioxane, toluene, H₂O, DMF, MeCN, and DCM. The results are presented in Fig. 7. It was found that organic bases such as DBU, DABCO and triethylamine showed better performance than inorganic bases,

probably due to their better solubility in the reaction system. Remarkably, DBU gave maximum conversion percentage. Moreover, base free conditions could not catalyze the reaction. The coupling reaction worked well in various organic solvents, but MeCN appeared to be the best choice amongst them. Negligible amount of product was formed when the reaction carried out in THF or hexane.

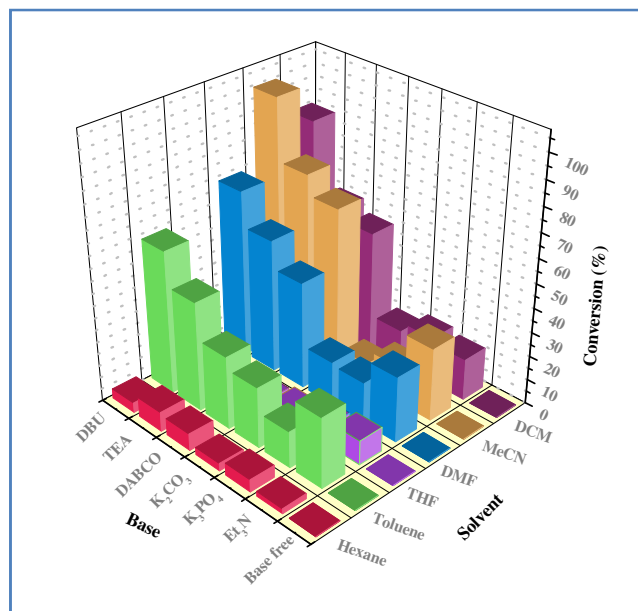


Fig. 7 Effect of solvents and bases on catalytic efficacy of SiO₂@APTES@DAFO-Fe in one pot three component coupling reaction (Reaction conditions: phenyl acetylene (1 mmol), dichloromethane (2 mmol), diethylamine (2 mmol), base (1 mmol), solvent (2 mL), catalyst (30 mg), temp. 70°C, time 10 h)

Effect of substrate molar ratio

Having established acetonitrile as the best solvent for three component coupling reaction, we then investigated the influence of substrate ratio and the results are summarized in Fig. 8.

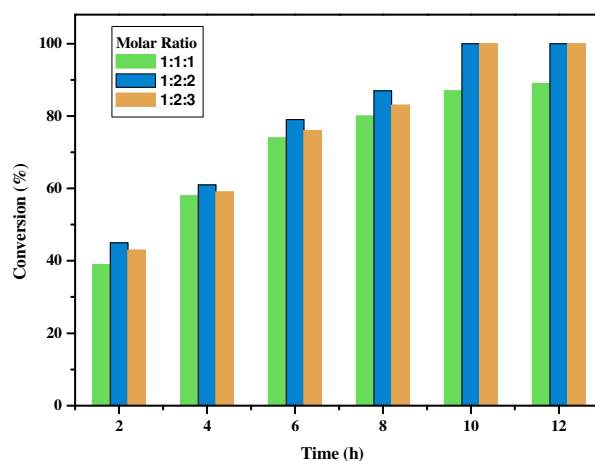


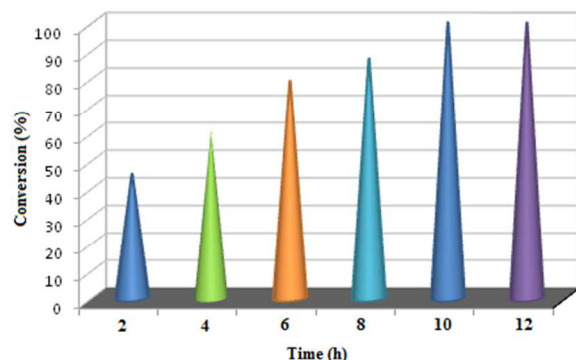
Fig. 8 Effect of substrate molar ratio on one pot three component coupling reaction (Reaction conditions: phenyl acetylene (a mmol), dichloromethane (b mmol), diethylamine (c mmol), DBU (1 mmol), solvent (2 mL), catalyst (30 mg), temp. 70°C, time 10 h)

Different molar ratios of phenylacetylene, dichloromethane and diethylamine (1:1:1, 1:2:2, and 1:2:3) were considered while keeping the other parameters fixed. Upon utilizing an equal molar ratio of the three substrates moderate conversion was observed.

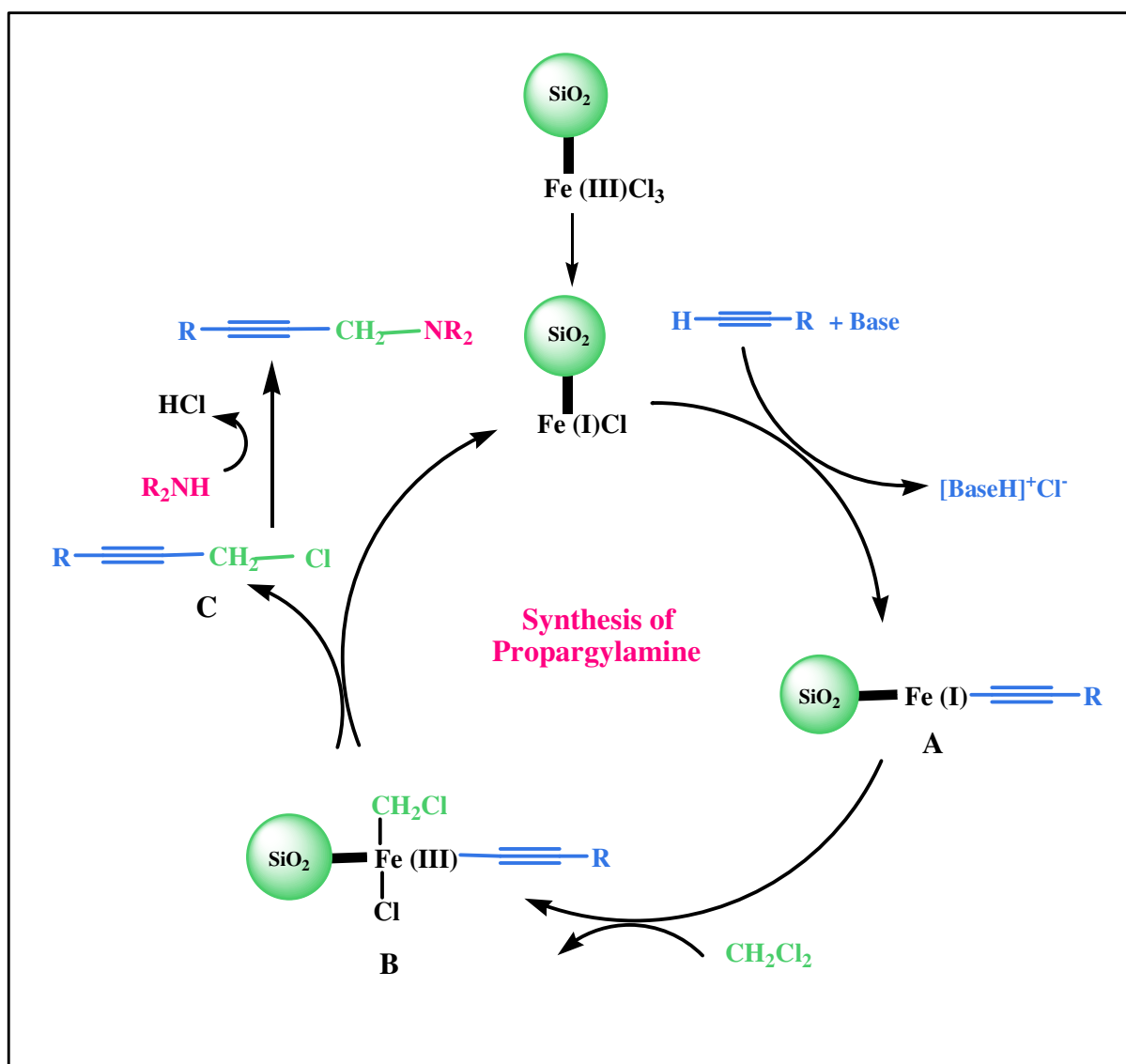
5 With further increase in the molar ratio of dichloromethane and diethylamine to 1:2:2, the reaction time was shortened and maximum conversion was observed. Hence, 1:2:2 molar ratio was the minimum requirement for the effective one pot synthesis of propargylamine. It was also observed that further increase in the molar ratio did not have any appreciable effect on the reaction conversion.

Effect of reaction time

Further, the percentage conversion of the model reaction was monitored at different reaction times. It can be seen from Fig. 9, 15 that with an increase in the reaction time, the percent conversion also increased upto 10 h. When the reaction was allowed to continue further, no significant change in the conversion was observed. So, the reaction time was optimized as 10 h.



20 **Fig. 9.** Effect of reaction time on one pot three component coupling reaction (Reaction conditions: phenyl acetylene (1 mmol), dichloromethane (2 mmol), diethylamine (2 mmol), DBU (1 mmol), solvent (2 mL), catalyst (30 mg), temp. 70°C)



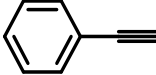
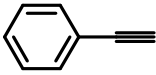
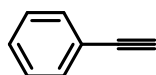
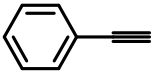
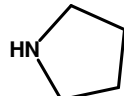
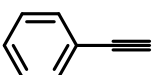
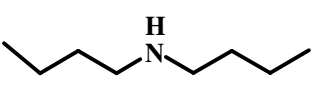
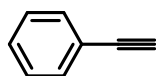
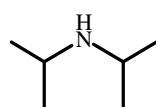
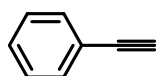
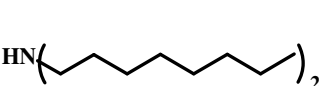
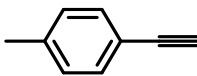
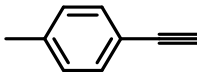
25 **Scheme 2** Probable reaction mechanism of SiO₂@APTES@DAFO-Fe catalyzed one pot three component coupling of terminal alkynes, dichloromethane and secondary amines.

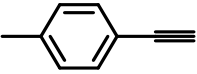
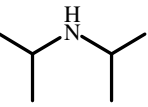
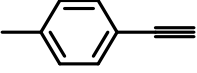
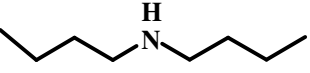
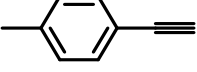
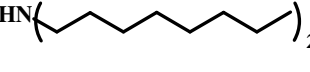
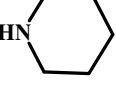
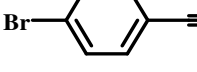
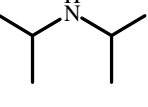
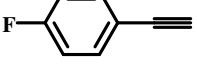
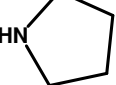
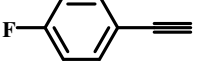
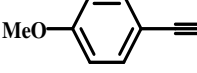
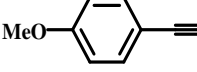
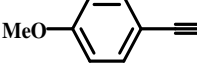
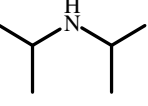
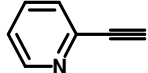
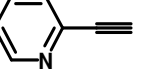
Cite this: DOI: 10.1039/c0xx00000x

www.rsc.org/xxxxxx

PAPER

Table 1 SiO₂@APTES@DAFO-Fe catalyzed one pot coupling reaction of terminal alkyne, dichloromethane and amines ^a.


S.No.	Alkyne	Dihalomethane	Amines	Time(h)	Conversion ^b (%)	Yield (%)
1.		CH ₂ Cl ₂		10	100	98
2.		CH ₂ Cl ₂		10	69	62
3.		CH ₂ Cl ₂		10	100	93
4.		CH ₂ Cl ₂		10	100	88
5.		CH ₂ Cl ₂		12	100	84
6.		CH ₂ Cl ₂		10	100	89
7.		CH ₂ Cl ₂		15	14	10
8.		CH ₂ Cl ₂		10	100	96
9.		CH ₂ Cl ₂		10	100	89

10.		CH ₂ Cl ₂		10	100	83
11.		CH ₂ Cl ₂		10	100	87
12.		CH ₂ Cl ₂		15	0	0
13.		CH ₂ Cl ₂		10	95	90
14.		CH ₂ Cl ₂		10	95	89
15.		CH ₂ Cl ₂		10	0	0
16.		CH ₂ Cl ₂		10	40	37
17.		CH ₂ Cl ₂		10	100	94
18.		CH ₂ Cl ₂		10	29	23
19.		CH ₂ Cl ₂		10	56	49
20.		CH ₂ Cl ₂		10	95	82
21.		CH ₂ Cl ₂		10	0	0
22.		CH ₂ Cl ₂		10	0	0

^a Reaction conditions: terminal acetylene (1 mmol), dichloromethane (2 mmol), secondary amine (2 mmol), acetonitrile (2 mL), DBU (1 mmol), catalyst (30 mg), temp. 70°C.

^b Conversions were determined by GC-MS.

Proposed reaction mechanism

A plausible mechanism for this coupling reaction has been proposed as shown in **Scheme 2**. Initially, precatalyst $\text{SiO}_2@\text{APTES}@DAFO\text{-Fe}$ might get reduced to a low-valent Fe(I) state in the presence of alkyne and base. The catalytic cycle starts via insertion of the C–H bond of the terminal alkyne promoted by Fe(I) species A in combination with DBU which leads to generation of a Fe-acetylide intermediate.^{63,64} The intermediate A thus formed acts as active nucleophilic species and reacts with CH_2Cl_2 to form the Fe(III) species B. Further, Fe(III) species B subsequently undergo reductive elimination to afford the propargylchloride C which upon reaction with a secondary amine yields corresponding propargylamine as product.^{39, 40, 65-67}

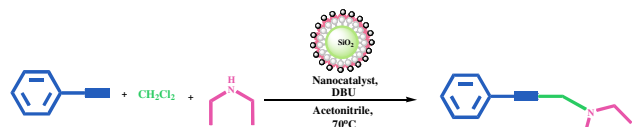
$\text{SiO}_2@\text{APTES}@DAFO\text{-Fe}$ catalyzed coupling reaction

In an effort to establish the scope of the protocol, we have assessed the catalytic activity of $\text{SiO}_2@\text{APTES}@DAFO\text{-Fe}$ under the optimized conditions for the synthesis of variety of propargylamine derivatives. For that, various terminal alkynes and secondary amine derivatives were subjected to coupling reaction to give a wide range of substituted propargylamines and results are summarized in **Table 1**. Both electron withdrawing and electron donating aromatic terminal alkynes afforded corresponding propargylamine products in good to excellent conversion percentage. However, in the case of heteroaromatic acetylene derivative such as ethynyl pyridine, negligible amount of product was obtained (**Table 1, entry 21 & 22**). Further, both cyclic and acyclic secondary amines such as piperidine, pyrrolidine, morpholine, diisopropylamine and dibutylamine were efficiently converted into the corresponding coupling products. Among these, dibutylamine required more time to complete the reaction (**Table 1, entry 5 & 11**). There was no reaction observed for bulky amines, such as dioctylamine which may be attributed to extra steric hindrance and lower nucleophilicity (**Table 1, entry 7 & 12**). The prominent feature of the present methodology was that this system had very good functional group tolerance for aromatic substituted alkynes and secondary amine derivatives.

Heterogeneity test

It is a well-known fact that stability and reusability are two important parameters based upon which a catalyst finds potential application in industry. In order to determine the true heterogeneous nature of Fe species in our catalytic system, standard leaching experiment was performed. For that, the model reaction was carried out under optimized reaction conditions employing $\text{SiO}_2@\text{APTES}@DAFO\text{-Fe}$ as catalyst. After 5 h, the reaction mixture was centrifuged to discharge $\text{SiO}_2@\text{APTES}@DAFO\text{-Fe}$ catalyst and subsequently permitted the remaining liquor to react for another 10 h. Then, GC-MS analysis of the supernatant was done and the results revealed that the conversion did not change with the increase in time, suggesting that the catalytic reactivity by the leaching iron metal could be excluded in the present coupling reaction (**Table 2**). Further, to ensure the absence of iron in the supernatant, UV-vis spectroscopic analysis was carried out and there was no characteristic peak of iron metal in the UV-vis spectrum of the supernatant. This was further confirmed by atomic adsorption analysis of the filtrate solution that showed no traces of iron in the supernatant after removal of the catalyst. Hence, it may be affirmed that silica nanospheres bind the iron metal very firmly

Table 2 Conversion percentage for coupling reaction of terminal alkyne, dichloromethane and amines under optimized conditions.



Entry	Time(h)	Conversion(%)	TON(TOF)
1 ^a	5	85	225(49)
2 ^b	10	85	225(49)

^a Reaction conditions: phenyl acetylene (1 mmol), dichloromethane (2 mmol), diethylamine (2 mmol), DBU (1 mmol) acetonitrile (2 mL), catalyst (30 mg), temp. 70°C

^b GC-MS analysis of supernatant after the removal of nano-catalyst.

and thus minimize the deterioration of the catalyst by reducing metal leaching which eventually facilitate efficient catalyst recycling.

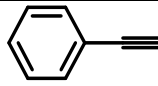
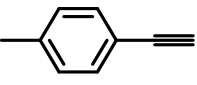
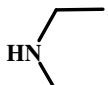
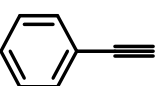
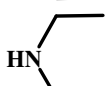
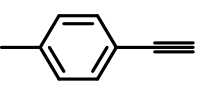
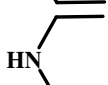
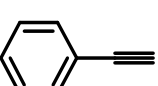
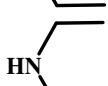
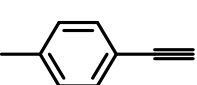
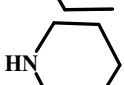
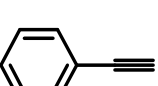
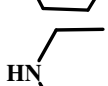
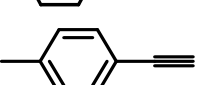
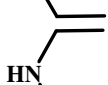
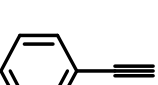
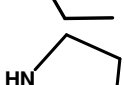
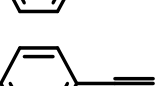
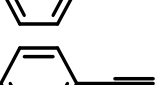
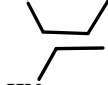
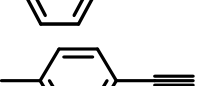
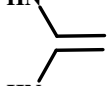
Reusability of catalyst

The easy catalyst recovery is a salient advantage of heterogeneous catalysis, allowing the metal reprocessing and even sometimes the catalyst recycling. To test the catalyst reusability, the reaction was carried out in the presence of a catalytic amount of $\text{SiO}_2@\text{APTES}@DAFO\text{-Fe}$ under the optimized reaction conditions (**Fig. 10**). Upon completion of the reaction, the catalyst was recovered, rinsed with ethyl acetate and dried under vacuum to eliminate any water trapped from moisture. Further, the recovered catalyst was redispersed in a freshly prepared reaction solution with other compositions identical to the initial run. Such recovery/ reinitiation cycles were repeated nine times. No remarkable decrease was observed in the catalytic activity after being used repetitively seven times, revealing its superiority over the corresponding homogeneous catalyst for reducing cost and diminishing environmental pollution from heavy metal ions. TEM and SEM image of the recovered catalyst did not show significant change in the morphology or in the size which indicates that the nanoarchitecture of the catalyst largely survived after reaction and recovery. Further, XRD patterns of recovered $\text{SiO}_2@\text{APTES}@DAFO\text{-Fe}$ were also compared with that of the fresh catalyst and it was found that both samples exhibited similar XRD patterns indicating that the catalyst was stable and could be regenerated for repeated use (**Fig. S2, ESI†**). Hence, silica nanospheres supported iron catalyst was proved to be a promising catalyst for one pot three component coupling reaction.

Comparison of the catalytic activity of the $\text{SiO}_2@\text{APTES}@DAFO\text{-Fe}$ nano-catalyst with the literature precedents.

The catalytic performance of the $\text{SiO}_2@\text{APTES}@DAFO\text{-Fe}$ was compared with that of the earlier reported catalytic systems for coupling reaction of terminal alkyne, dihalomethane and amines. As evident from **table 3**, the $\text{SiO}_2@\text{APTES}@DAFO\text{-Fe}$ catalyst exhibited much better results in terms of catalytic activity, reaction conditions and superior reusability in comparison to the literature precedents. This may be due to the high surface to volume ratio of the nano-catalyst in comparison to the bulk catalytic systems. It should also be noted that most of the reported catalyst were homogeneous and hence decomposed immediately

Table 3 Comparison of the catalytic activity of SiO₂@APTES@DAFO-Fe nano-catalyst with other catalysts reported in literature for one pot coupling reaction of terminal alkyne, dihalomethane and amines.

Entry	Acetylene	Halomethane	Amines	Reaction Conditions	Time (h)	Reusability	Yield (%)	Reference
1.		CH ₂ Cl ₂		Ni(Py) ₄ Cl ₂ / Bipyridine/ MeCN 70°C	28	-	92	[39]
2.		CH ₂ Cl ₂		Ni(Py) ₄ Cl ₂ / Bipyridine/ MeCN 70°C	28	-	90	[39]
3.		CH ₂ Cl ₂		CoBr ₂ , DBU, MeCN, 80°C	30	-	85	[40]
4.		CH ₂ Cl ₂		CoBr ₂ , DBU, MeCN, 80°C	30	-	88	[40]
5.		CH ₂ Cl ₂		FeCl ₃ , TMG, MeCN, 100°C	12	-	67	[41]
6.		CH ₂ Cl ₂		FeCl ₃ , TMG, MeCN, 100°C	12	-	88	[41]
7.		CH ₂ Cl ₂		CuCl, DBU, 60°C	14	-	95	[42]
8.		CH ₂ Cl ₂		CuCl, DBU, 60°C	14	-	94	[42]
9.		CH ₂ Cl ₂		nano In ₂ O ₃ DABCO DMSO, 65 °C	20	Upto 3 catalytic cycles	72	[43]
10.		CH ₂ Cl ₂		nano In ₂ O ₃ DABCO DMSO, 65 °C	16	Upto 3 catalytic cycles	80	[43]
11.		CH ₂ Cl ₂		DBU, acetonitrile, SiO ₂ @APTES@DAFO-Fe, 70°C	10	Upto 7 catalytic cycles	98	Present study
12.		CH ₂ Cl ₂		DBU, acetonitrile, SiO ₂ @APTES@DAFO-Fe, 70°C	10	Upto 7 catalytic cycles	96	Present study

after the reaction and could not be reused. Moreover, it is necessary to remove toxic metals from the final product as metal contamination is highly regulated, especially in the pharmaceutical industry. There is only one report in literature wherein expensive indium oxide was used as catalyst for the concerned reaction and could be repeatedly used for three consecutive cycles. On the other hand, the reusability of the developed SiO₂@APTES@DAFO-Fe catalyst has been demonstrated for seven cycles without any appreciable loss of its catalytic activity.

Conclusion

In conclusion, a novel silica nanospheres supported iron catalyst

has been synthesized via grafting of diazafluorene ligand onto amine functionalized silica nanospheres followed by metallation with ferric chloride. The prepared catalyst has been found to be highly efficient for the one pot synthesis of propargylamines from alkynes, aldehydes, and amines. The methodology is quite simple and allows the synthesis of a diverse range of propargylamines in good to excellent yields. The activity of the nano-catalyst is found to be superior in terms of reaction time, yield, cost, selectivity and reusability as compared to literature precedents. This may be ascribed to the nanometre size of silica nanospheres which enhances the dispersion of the catalytic active sites in the reaction medium and thus improving their accessibility to the substrate and base species. Further, the

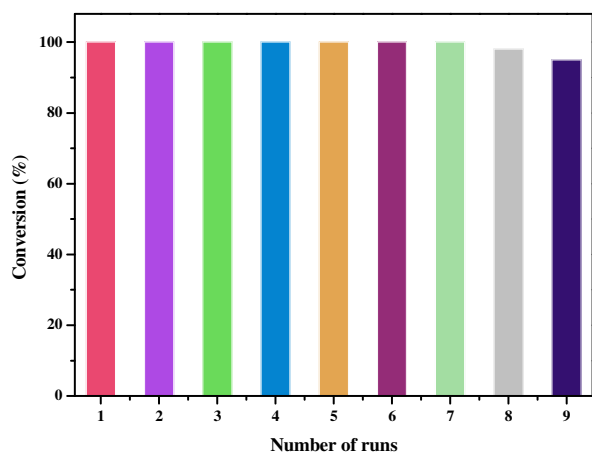


Fig. 10 Catalytic reusability test for one pot three component coupling reaction (reaction conditions: phenyl acetylene (1 mmol), dichloromethane (2 mmol), diethylamine (2 mmol), DBU (1 mmol), acetonitrile (2 mL), catalyst (30 mg), temp. 70°C, time 10 h)

nanocatalyst can be easily recovered by centrifugation and reused several times without any significant decay in its activity, thereby making this protocol environmentally benign. The heterogeneity test provides an excellent evidence for the absence of leaching of the active catalytic species which results in excellent durability of the catalyst under present experimental conditions. The synthetic protocol is straightforward, safe, environmentally clean, and free from any other additives and thus abides by a number of principles of green chemistry. Some of the other advantages of the present methodology are ease of preparation of the catalyst from commercially available starting materials, simple work-up procedure, high product yield, easy recovery and reusability of the catalyst for several cycles with unaltered activity and selectivity. Consequently, this methodology offers a new approach for the synthesis of propargylamines using silica nanospheres supported iron catalyst for the first time under mild reaction conditions.

References

1. A. R. Sheldon, *Chem. Soc. Rev.*, 2012, **41**, 1437-1451.
2. A. Corma and H. Garcia, *Catal. Today*, 1997, **38**, 257-308.
3. M. H. Valkenberg and W. F. Holderich, *Catal. Rev. Sci. Eng.*, 2002, **44**, 321-374.
4. A. Corma and H. Garcia, *Adv. Synth. Catal.*, 2006, **348**, 1391-1412.
5. J. M. Fraile, J. I. Garcia and J. A. Mayoral, *Chem. Rev.*, 2009, **109**, 360-417.
6. A. Zamboulis, N. Moitra, J. J. E. Moreau, X. Cattoen and M. W. C. Man, *J. Mater. Chem.*, 2010, **20**, 9322-9338.
7. B. C. Gates, *Chem. Rev.*, 1995, **95**, 511-522.
8. A. Corma and H. Garcia, *Adv. Synth. Catal.*, 2006, **348**, 1391-1412.
9. J. C. Hicks, B. A. Mullis, C. W. Jones, *J. Am. Chem. Soc.* 2007, **129**, 8426-8427.
10. N. T. S. Phan and C. W. Jones, *J. Mol. Catal. A: Chem.*, 2006, **253**, 123-131.
11. J.-Y. Park, Y.-J. Lee, P. K. Khanna, K.-W. Jun, J. W. Bae and Y. H. Kim, *J. Mol. Catal. A: Chem.*, 2010, **323**, 84-90.
12. A. F. Trindade, P. M. P. Gois and C. A. M. Afonso, *Chem. Rev.*, 2009, **109**, 418-514.
13. M. Moghadama, S. Tangestaninejada, V. Mirkhania, I. M. Baltorka, A. Mirjafari and N. S. Mirbagheria, *J. Mol. Catal. A: Chem.*, 2010, **329**, 44-49.

14. C. Pereira, A.R. Silva, A. P. Carvalho, J. Pires and C. Freire, *J. Mol. Catal. A: Chem.*, 2008, **283**, 5-14.
15. C. Pereira, K. Biernacki, S. L. H. Rebelo, A. L. Magalhaes, A. P. Carvalho, J. Pires and C. Freire, *J. Mol. Catal. A: Chem.*, 2009, **312**, 53-64.
16. S. Miao, C. Zhang, Z. Liu, B. Han, Y. Xie, S. Ding and Z. Yang, *J. Phys. Chem. C*, 2008, **112**(3), 774-780.
17. S. Yu, H. J. Yun, D. M. Lee and J. Yi, *J. Mater. Chem.*, 2012, **22**, 12629-12635.
18. N. Suzuki, J. Yu, N. Shioda, H. Asami, T. Nakamura, T. Huhn, A. Fukuoka, M. Ichikawa, M. Saburi and Y. Wakatsuki, *Appl. Catal., A*, 2002, **224**, 63-75.
20. B. Yuan, X. He, Y. Chen and K. Wang, *Macromol. Chem. Phys.*, 2011, **212**, 2378-2388.
21. H. E. Bergna and W. O. Roberts, *Colloidal Silica: Fundamentals and Applications*, CRC Press, Taylor & Francis, Boca Raton, USA, 2006.
22. I. I. Slowing, B. G. Trewyn, S. Giri and V. S.-Y. Lin, *Adv. Funct. Mater.*, 2007, **17**, 1225-1236.
23. I. I. Slowing, J. L. Vivero-Escoto, B. G. Trewyn and V. S.-Y. Lin, *J. Mater. Chem.*, 2010, **20**, 7924-7937.
24. M. Pagliaro, R. Ciriminna and G. Palmisano, *J. Mater. Chem.*, 2009, **19**, 3116-3126.
25. J. M. Rosenholm, C. Sahlgren and M. Linden, *Nanoscale*, 2010, **2**, 1870-1883.
26. W. He, F. Zhang and H. Li, *Chem. Sci.*, 2011, **2**, 961-966.
27. R. H.-Y. Chang, J. Jang and K. C.-W. Wu, *Green Chem.*, 2011, **13**, 2844-2850.
28. X. Du and J. He, *Nanoscale*, 2012, **4**, 852-859.
29. S. Banerjee, J. Das, R. P. Alvarez and S. Santra, *New J. Chem.*, 2010, **34**, 302-306.
30. H.-T. Chen, S. Huh, J. W. Wiench, M. Pruski and V. S.-Y. Lin, *J. Am. Chem. Soc.*, 2005, **127**, 13305-13311.
31. P. Veerakumar, M. Velayudham, K.-L. Lub and S. Rajagopal, *Catal. Sci. Technol.*, 2011, **1**, 1512-1525.
32. M. A. Huffman, N. Yasuda, A. E. DeCamp and E. J. J. Grabowski, *J. Org. Chem.*, 1995, **60**, 1590-1594.
33. M. Konishi, H. Ohkuma, T. Tsuno, T. Oki, G. D. VanDuyne and J. Clardy, *J. Am. Chem. Soc.*, 1990, **112**, 3715-3716.
34. M. Miura, M. Enna, K. Okuro and M. Nomura, *J. Org. Chem.*, 1995, **60**, 4999-5004.
35. A. Jenmalm, W. Berts, Y. L. Li, K. Luthman, I. Csoregh and U. Hacksell, *J. Org. Chem.*, 1994, **59**, 1139-1148.
36. G. Dyker, *Angew. Chem., Int. Ed.*, 1999, **38**, 1698-1712.
37. T. Naota, H. Takaya and S. I. Murahashi, *Chem. Rev.*, 1998, **98**, 2599-2660.
38. D. Aguilar, M. Contel and E. P. Urriolabeitia, *Chem. Eur. J.*, 2010, **16**, 9287-9296.
39. S. R. Lanke and B. M. Bhanage, *Appl. Organometal. Chem.*, 2013, **27**, 729-733.
40. Y. Tang, T. Xiao, Lei, *Tetrahedron Lett.*, 2012, **53**, 6199-6201.
41. J. Gao, Q.-W. Song, L.-N. He, Z.-Z. Yang and X.-Y. Dou, *Chem. Commun.*, 2012, **48**, 2024-2026.
42. D. Yua and Y. Zhang, *Adv. Synth. Catal.*, 2011, **353**, 163-169.
43. M. Rahman, A. K. Bagdi, A. Majee, A. Hajra, *Tetrahedron Lett.*, 2011, **52**, 4437-4439.
44. Z. Lin, D. Yu, Y. Zhang, *Tetrahedron Lett.* 2011, **52**, 4967-4970.
45. R. K. Sharma and S. Sharma, *Dalton Trans.*, 2014, **43**, 1292-1304.
46. R. Sharma and S. Dhingra, *Designing and Synthesis of Functionalized Silica Gels and their Applications as Metal Scavengers, Sensors, and Catalysts: A Green Chemistry Approach*, LAP Lambert Academic Publishing LAP Lambert Academic Publishing, Germany, 2011.
47. R. K. Sharma, A. Puri, Y. Monga and A. Adholeya, *J. Mater. Chem. A*, 2014, **2**, 12888-12898.
48. R. K. Sharma, Y. Monga, A. Puri and G. Gaba, *Green Chem.*, 2013, **15**, 2800-2809.
49. R. K. Sharma, S. Sharma, S. Gulati and A. Pandey, *Anal. Methods*, 2013, **5**, 1414-1426.
50. R. K. Sharma, Y. Monga and A. Puri, *Catal. Commun.*, 2013, **35**, 110-114.
51. R. K. Sharma, S. Gulati, A. Pandey and A. Adholeya, *Appl. Catal., B*, 2012, **125**, 247-258.

52. R. K. Sharma and Y. Monga, *Appl. Catal., A.*, 2013, **454**, 1-10.
53. R. K. Sharma, A. Pandey, S. Gulati and A. Adholeya, *J. Hazard. Mater.*, 2012, **209-210**, 285-292.
54. R. K. Sharma, D. Rawat and G. Gaba, *Catal. Commun.*, 2012, **19**, 31-36.
55. R. K. Sharma and S. Gulati, *J. Mol. Catal. A: Chem.*, 2012, **363-364**, 291-303.
56. R. K. Sharma and P. Pant, *J. Hazard. Mater.*, 2009, **163**, 137-142.
57. R. K. Sharma and C. Sharma, *Catal. Commun.*, 2011, **12**, 327-331.
58. Y. He and X. Yu, *Mater. Lett.*, 2007, **61**, 2071-2074.
59. V. Mahalingam, S. Onclin, M. Peter, B. J. Ravoo, J. Huskens and D. N. Reinhoudt, *Langmuir*, 2004, **20**, 11756-11762.
60. D. Tang, L. Zhang, Y. Zhang, Z.-A. Qiao, Y. Liu and Q. Huo, *J. Colloid Interface Sci.*, 2012, **369**, 338-343.
61. K. B. Sidhuria, A. L. Daniel-da-Silva, T. Trindade and J. A. P. Coutinho, *Green Chem.*, 2011, **13**, 340-349.
62. C. Pereira, J. F. Silva, A. M. Pereira, J. P. Araujo, G. Blanco, J. M. Pintadoc and C. Freire, *Catal. Sci. Technol.*, 2011, **1**, 784-793.
63. Y. Nakajima, Y. Nakao, S. Sakaki, Y. Tamada, T. Ono, and F. Ozawa, *J. Am. Chem. Soc.*, 2010, **132**, 9934-9936.
64. C.J. Adams, R.B. Bedford, E. Carter, N.J. Gower, M.F. Haddow, J.N. Harvey, M. Huwe, M. A. Cartes, S.M. Mansell, C. Mendoza, D.M. Murphy, E.C. Neeve, and J. Nunn, *J. Am. Chem. Soc.*, 2012, **134**, 10333-10336.
65. V. Yempally, S. Moncho, S. Muhammad, E.N. Brothers, B.A. Arndtsen, and A.A. Bengali, *Organometallics*, 2014, **33**, 3591-3595.
66. J.Y. Zeng, M.-H. Hsieh, H.M. Lee, *J. Organomet. Chem.*, 2005, **690**, 5662-5671.
67. H. Nishiyama, M. Horihata, T. Hirai, S. Wakamatsu, and K. Itoh, *Organometallics*, 1991, **10**, 2708-2717.